

# Chaos Analysis of a Fuel-Slosh Coupled Aircraft System

Ons Kooli <sup>1</sup> and İhsan Pehlivan <sup>2</sup>

\*Sakarya University of Applied Sciences, Faculty of Technology, Department of Electrical and Electronics Engineering, Sakarya, Türkiye.

**ABSTRACT** This study investigates nonlinear and chaotic dynamics induced by fuel sloshing in a partially filled aircraft tank. The system is modeled as a rigid aircraft pitch degree of freedom coupled with a nonlinear slosh pendulum, representing the dominant liquid motion. Numerical simulations are used to analyze the system response through time series and phase portraits, revealing complex dynamical behavior. Chaotic dynamics are quantitatively confirmed using Lyapunov exponents and their parametric variation. In addition, bifurcation analyses are performed with respect to key system parameters, illustrating transitions from periodic to chaotic motion. The results highlight the significant impact of fuel slosh on aircraft pitch dynamics and emphasize the importance of accounting for nonlinear fluid–structure interactions in stability analysis and control-oriented modeling.

## KEYWORDS

Nonlinear dynamics  
Fuel sloshing  
Aircraft pitch dynamics  
Chaotic motion  
Dynamical analysis

## INTRODUCTION

Understanding nonlinear interactions in aircraft systems is crucial for both control performance and flight safety. One important source of nonlinear behavior is fuel slosh, where the motion of liquid inside partially filled tanks couples with the rigid-body dynamics of the aircraft. This coupling can introduce additional forces and moments that significantly alter the system response, potentially leading to large oscillations, loss of stability, or even chaotic motion under relatively small excitations. Recent studies have emphasized that such nonlinearities are not merely secondary effects but can be primary drivers of complex instability in modern aerospace structures (Mahmoudvand *et al.* 2025).

Fuel sloshing dynamics are particularly relevant for large aircraft, launch vehicles, and unmanned aerial vehicles with significant fuel volumes. The pendulum-like motion of liquid with a free surface can amplify pitching, rolling, or yawing oscillations and modify the effective inertia and damping of the vehicle. Extensive research has investigated the hydrodynamic aspects of sloshing and its interaction with structural dynamics, highlighting its influence on stability, loads, and energy dissipation mechanisms (Faltinsen 2005; Ibrahim 2005). Experimental and numerical studies in aerospace applications have shown that fuel slosh can alter

dynamic responses and aeroelastic characteristics depending on fill level, excitation frequency, and tank geometry (Constantin *et al.* 2022; Langlois and Kabamba 2015; Wang *et al.* 2021). Recent advancements in bifurcation analysis have further revealed that even subtle changes in flight parameters can trigger abrupt transitions in coupled fluid-structure systems (Liu and Wang 2024).

To model sloshing effects efficiently, many works have employed reduced-order mechanical analogs, such as pendulum or mass–spring representations, to approximate liquid motion without resorting to full computational fluid dynamics simulations. These simplified models have been successfully applied in spacecraft attitude dynamics and aircraft fuel tank studies, providing valuable insight into slosh-induced forces and moments while maintaining analytical and computational tractability (Schlee and Smith 2006; Savella and Ibrahim 2005; Reyhanoglu and van der Schaft 2011). Current research continues to utilize these analogs to develop robust control strategies capable of suppressing nonlinear oscillations in real-time (Chen and Zhang 2025).

Despite these advances, most existing studies focus on linearized behavior, stability margins, or damping characteristics. Comparatively fewer works explicitly address the nonlinear and chaotic dynamics that may arise from the coupling between rigid-body motion and fuel slosh under periodic excitation. Phenomena such as sensitivity to initial conditions, aperiodic oscillations, and transitions to chaos remain insufficiently explored in coupled pitch–slosh systems.

Manuscript received: 30 October 2025,

Revised: 23 December 2025,

Accepted: 11 January 2026.

<sup>1</sup>onskooli@zohomail.eu (Corresponding author).

<sup>2</sup>ipehlivan@subu.edu.tr

Motivated by this gap, the present work investigates a nonlinear aircraft pitch model coupled with a fuel slosh pendulum. The system dynamics are analyzed through equilibrium analysis, Jacobian and eigenvalue evaluation, time-series responses, phase portraits, Lyapunov exponents and spectra, as well as bifurcation diagrams. Parameter variations are explored to study their influence on system stability and chaotic behavior. The results demonstrate that fuel slosh can act as a source of strong nonlinearity capable of inducing complex and chaotic responses, emphasizing the importance of accounting for such effects in aircraft dynamic analysis, stability assessment, and control design.

## DESCRIPTION OF THE COUPLED SYSTEM

In this study, the aircraft is modeled as a rigid body undergoing pitch motion and coupled with a simplified fuel slosh representation. The liquid motion inside the fuel tank is approximated using a mechanical analog in the form of a pendulum, which captures the dominant sloshing mode associated with the free-surface motion of the fuel. This reduced-order approach allows the essential nonlinear coupling between the aircraft pitch dynamics and the internal fuel motion to be analyzed without resorting to full fluid dynamic simulations.

The coupling between the aircraft and the sloshing fuel introduces additional forces and moments that act on the pitching motion, modifying the effective inertia, damping, and stiffness of the system. Conversely, the aircraft pitch acceleration influences the slosh dynamics, resulting in a bidirectional interaction. Such mutual coupling is a known source of nonlinear behavior and may lead to complex dynamic responses, including quasiperiodic and chaotic oscillations under certain excitation conditions.

The resulting mathematical model consists of a set of nonlinear ordinary differential equations governing the aircraft pitch angle and rate, together with the angular displacement and velocity of the slosh pendulum. These equations form the basis for the analytical and numerical investigations presented in the subsequent sections.

While the single-pendulum mechanical analog effectively captures the dominant longitudinal sloshing mode and the resulting chaotic transitions, it is acknowledged that more complex approximations can provide higher-order fidelity. Advanced modeling techniques, such as multi-pendulum arrays, hydraulic mechanical models, or high-fidelity Computational Fluid Dynamics (CFD) simulations, can capture additional slosh modes and secondary nonlinearities arising from fluid viscosity and complex tank geometries. However, for the purpose of investigating the fundamental mechanisms of chaos and bifurcations in pitch-slosh coupling, the reduced-order pendulum model provides a computationally efficient and analytically tractable framework that preserves the essential nonlinearities of the system.

### Aircraft Control and Pitch Dynamics

To understand the forced pitch-actuator system analyzed in this study, it is important to review the primary control surfaces and their influence on aircraft motion. Figure 1 illustrates a schematic of a generic fixed-wing aircraft, showing the elevator, rudder, and ailerons.

Pitch and Elevator, Pitch refers to the rotation of the aircraft about its lateral axis (nose up or nose down). The *elevator*, located on the horizontal tail, is the primary control surface that commands this motion. Moving the elevator up causes the nose to rise (positive pitch), while moving it down causes the nose to drop (negative pitch).

Aircraft Primary Control Surfaces and Rotational Axes

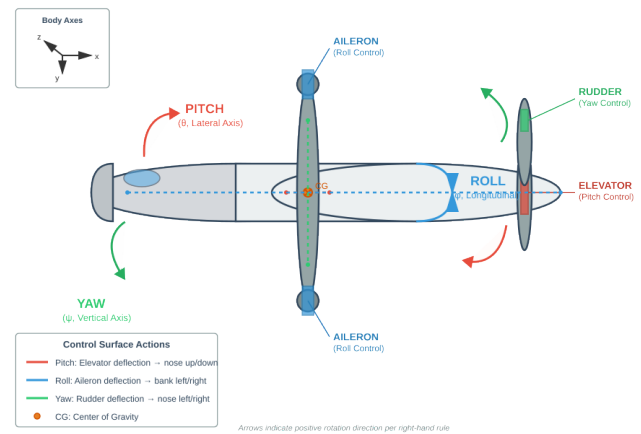


**Figure 1** Schematic of a fixed-wing aircraft showing primary control surfaces and rotational axes: pitch (elevator), roll (ailerons), and yaw (rudder).

Roll and Ailerons, Roll is the rotation about the longitudinal axis of the aircraft. The *ailerons*, located on the trailing edge of the wings, control roll. Deflecting one aileron up and the other down causes the aircraft to tilt sideways, enabling banking turns.

Yaw and Rudder, Yaw is the rotation about the vertical axis, controlling the left-right direction of the nose. The *rudder*, mounted on the vertical tail fin, produces yawing moments. Moving the rudder left or right rotates the aircraft nose in the corresponding direction.

In this work, the forced nonlinear system models the coupling between the aircraft pitch and the elevator dynamics under periodic forcing. The pitch stiffness is characterized by a cubic nonlinearity, modeled as a Duffing-type oscillator. Understanding these basic control surfaces and their associated motions is crucial for interpreting the system's response, including quasi-periodic and chaotic behaviors.

The system consists of:

- A rigid aircraft with pitch degree of freedom  $\theta$ , modeled with a Duffing-type cubic nonlinear stiffness.
- A partially filled fuel tank, modeled as a pendulum mass  $m_s$  of length  $l$  and slosh damping  $c_s$ .
- Nonlinear coupling between aircraft pitch acceleration and slosh motion via coupling coefficient  $\beta$ .
- Optional external periodic forcing representing aerodynamic gusts or engine vibrations.

### Physical Explanation

The slosh mass acts like a pendulum whose motion is affected by the aircraft pitch  $\theta$  and, in turn, applies a nonlinear torque to the aircraft. This coupling introduces a strong source of nonlinearity through the interaction of the state variables and parameters. Specifically, the aircraft's longitudinal motion is defined by the pitch angle  $\theta$  and angular rate  $q = \dot{\theta}$ , while the internal liquid dynamics are represented by the slosh pendulum angle  $\phi$  and its rate  $\psi = \dot{\phi}$ .

The system's complexity arises from the nonlinear coupling where the aircraft acceleration  $\ddot{\theta}$  influences the slosh motion via the coupling coefficient  $\beta$ , and the resulting slosh displacement feeds back as a corrective or perturbing torque on the pitch dynamics

## Aircraft-Fuel Slosh Coupling Dynamics

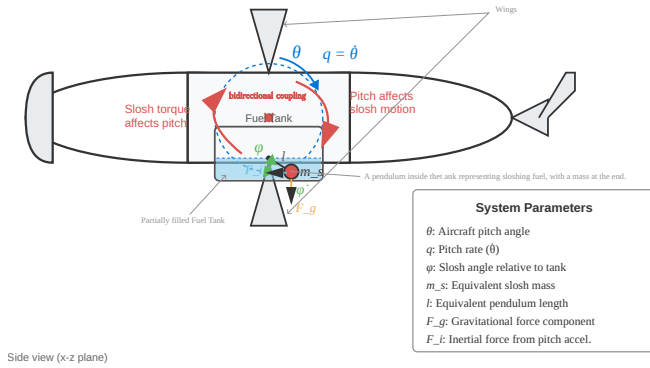


**Figure 2** Schematic of aircraft coupled with a slosh pendulum representing fuel motion.

through the coefficient  $K_c$ . Furthermore, the energy dissipation in the system is governed by the aircraft's aerodynamic damping ratio  $\zeta$  and the slosh-specific damping coefficient  $c_s$ ; however, while these terms reduce total energy, they do not eliminate the potential for complex aperiodic behavior or the onset of chaos.

### Fuel Tank Dynamics

The aircraft considered in this study contains a partially filled fuel tank, which introduces additional nonlinear effects due to fluid motion. The tank is typically located near the center of mass of the aircraft to minimize static stability issues; however, the dynamic motion of the liquid can generate significant forces that affect the airframe's response. For modeling purposes, the tank geometry is assumed to be rigid, possessing a rectangular or cylindrical shape. The fuel inside this volume is allowed to move freely, generating sloshing waves in response to both the aircraft's linear acceleration and rotational pitch maneuvers. In this study, the slosh degrees of freedom are primarily restricted to the longitudinal (nose–tail) direction, as this provides the most direct and significant coupling with the aircraft's pitch dynamics, whereas lateral slosh is neglected to maintain a focused analysis on longitudinal stability.

### Coupling Between Aircraft Pitch and Fuel Slosh

The motion of the fuel inside the tank interacts with the aircraft dynamics, introducing nonlinear coupling between the pitch-actuator system and the fluid motion. When the aircraft undergoes a pitch maneuver, the free surface of the fuel tilts, generating additional forces and moments that act upon the aircraft's center of mass. These slosh-induced forces subsequently modify the pitch trajectory and can excite unwanted oscillations throughout the airframe. Under specific conditions of periodic external forcing, the recursive interaction between the aircraft pitch and the internal fuel slosh can lead to highly complex dynamics, including quasi-periodic transitions or fully developed chaotic behavior.

## FUEL SLOSH MODEL AND GOVERNING DYNAMICS

The coupled aircraft pitch and fuel-slosh dynamics are modeled as a nonlinear four-dimensional system. The state variables are the

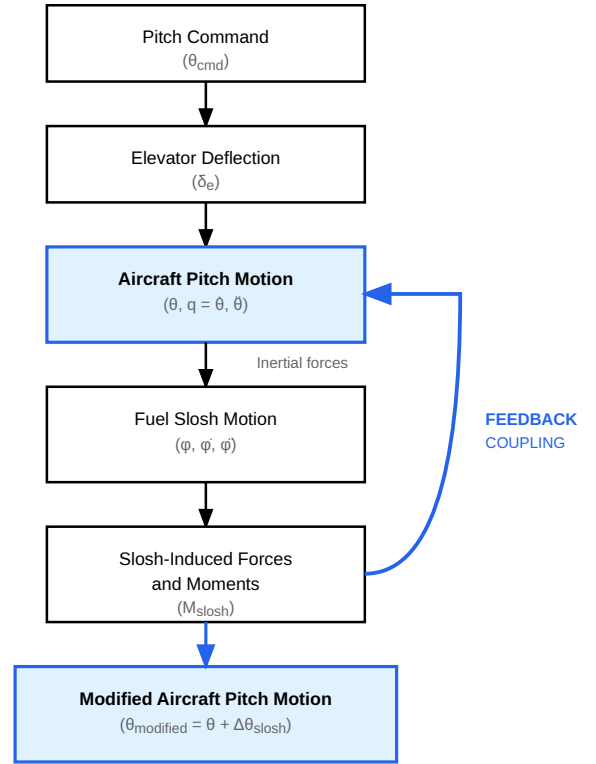


**Figure 3** Computational framework and feedback coupling logic between the aircraft pitch control and the nonlinear fuel slosh dynamics.

aircraft pitch angle  $\theta$ , pitch rate  $q$ , slosh displacement  $\phi$ , and slosh velocity  $\dot{\phi}$ .

The pitch dynamics are modeled using a Duffing-type nonlinear oscillator with external harmonic excitation, a formulation commonly adopted in vibration and chaos studies of mechanical and aeroelastic systems (Beltrán-Carbajal and Silva-Navarro 2009).

$$\begin{aligned}\dot{\theta} &= q, \\ \dot{q} &= -\omega_n^2\theta + \alpha\theta^3 - 2\zeta\omega_n q + K_c\phi + F\sin(\omega t), \\ \dot{\phi} &= \psi, \\ \dot{\psi} &= -\omega_s^2\phi - c_s\psi - \beta\dot{q},\end{aligned}\quad (1)$$

where  $\omega_s$  is the natural frequency of the slosh pendulum and  $c_s$  is the slosh damping coefficient. In the numerical implementation, the expression for  $\dot{q}$  is substituted into the  $\dot{\psi}$  equation to decouple the accelerations and form an explicit state-space representation. This substitution reveals the direct influence of the nonlinear pitch stiffness and aerodynamic damping on the fuel slosh acceleration.

The numerical simulations are conducted using a set of dimensionless parameters that represent a realistic physical configuration of a mid-sized transport aircraft. The mass ratio between the sloshing fuel and the aircraft ( $m_s/m_b$ ), the pendulum length ( $l$ ), and the damping coefficients ( $\zeta, c_s$ ) are selected to align with experimental benchmarks and literature-based values for longitudinal slosh dynamics (Ibrahim 2005; Faltinsen and Timokha 2009). Specifically, the use of a pendulum analog to represent the first sloshing mode

**Table 1** State variables and parameters synchronized with the numerical simulation results

| Symbol     | Meaning                                  | Value (in Code) |
|------------|--|-----------------|
| $\theta$   | Aircraft pitch angle (rad)               | variable        |
| $q$        | Pitch rate (rad/s)                       | variable        |
| $\phi$     | Slosh displacement angle (rad)           | variable        |
| $\psi$     | Slosh angular rate (rad/s)               | variable        |
| $\omega_n$ | Aircraft pitch natural frequency (rad/s) | 1.0             |
| $\zeta$    | Aerodynamic damping ratio                | 0.02            |
| $\alpha$   | Nonlinear pitch stiffness coefficient    | 1.0             |
| $\omega_s$ | Slosh natural frequency (rad/s)          | 1.8             |
| $c_s$      | Slosh damping coefficient                | 0.05            |
| $\beta$    | Pitch-to-slosh coupling coefficient      | 1.2             |
| $K_c$      | Slosh-to-pitch coupling coefficient      | 0.6             |
| $F$        | Forcing amplitude                        | 0.4             |
| $\omega$   | Forcing frequency (rad/s)                | 1.1             |

is a well-established method validated by the experimental studies of Ibrahim (Ibrahim 2005) and Faltinsen (Faltinsen and Timokha 2009), ensuring that the observed chaotic transitions occur within physically meaningful operational regimes.

The specific state variables and structural parameters governing the system's behavior are summarized in Table 1. Building upon this framework, the term  $F \sin(\omega t)$  represents an external harmonic excitation acting on the aircraft pitch dynamics. Such periodic forcing is commonly employed to model oscillatory aerodynamic loads, control surface actuation, or the impact of atmospheric turbulence on the longitudinal stability. The term  $F \sin(\omega t)$  represents an external harmonic excitation acting on the aircraft pitch dynamics. Such periodic forcing is commonly employed to model oscillatory aerodynamic loads, control surface actuation, or base excitation of fuel tanks. Sinusoidal excitation is widely used in nonlinear slosh–structure interaction and aircraft dynamics studies, as it provides a bounded and analytically tractable input that facilitates the investigation of nonlinear resonance, bifurcations, and chaotic responses (Nayfeh and Mook 1979; Ibrahim 2005; Faltinsen and Timokha 2009). While other forms of excitation may be considered, harmonic forcing serves as a canonical baseline for nonlinear dynamic analysis.

The initial conditions of the system are:

$$\theta_0 = 0.05, \quad q_0 = 0, \quad \phi_0 = 0.02, \quad \psi_0 = 0.$$

### Equilibrium States and Stability Analysis

Equilibrium points of the coupled aircraft–fuel slosh system are obtained by setting all time derivatives equal to zero. The state vector is defined as

$$\mathbf{x} = [\theta, q, \phi, \psi]^T,$$

where  $\theta$  is the aircraft pitch angle,  $q = \dot{\theta}$  is the pitch rate,  $\phi$  is the slosh pendulum angle, and  $\psi = \dot{\phi}$  is its angular rate.

For equilibrium analysis, the autonomous form of the system is considered by neglecting the external forcing term ( $F = 0$ ). An equilibrium state  $\mathbf{x}^*$  therefore satisfies

$$\dot{\theta} = \dot{q} = \dot{\phi} = \dot{\psi} = 0.$$

From Eqs. (1), these conditions immediately yield

$$q^* = 0, \quad \psi^* = 0.$$

The remaining equilibrium conditions are obtained from the pitch and slosh acceleration equations, which reduce to the coupled algebraic system

$$\begin{aligned} -\omega_n^2 \theta^* + \alpha(\theta^*)^3 - K_c \phi^* &= 0, \\ -\omega_s^2 \phi^* - \beta \theta^* &= 0. \end{aligned} \quad (2)$$

Besides the trivial equilibrium at the origin  $(\theta^*, \phi^*) = (0, 0)$ , the nonlinear term  $\alpha \theta^3$  allows for the existence of nonzero equilibrium solutions. Solving Eq. (2) yields two symmetric equilibrium points of the form

$$\theta^* = \pm \theta_e, \quad \phi^* = \mp \phi_e,$$

where  $\theta_e > 0$  and  $\phi_e > 0$  denote the magnitudes of the equilibrium pitch angle and slosh angle, respectively. Note that the slosh angle  $\phi^*$  has an opposite sign to  $\theta^*$  due to the coupling term.

Consequently, the system admits two symmetric nontrivial equilibrium points given by

$$E_{\pm} = (\pm \theta_e, 0, \mp \phi_e, 0).$$

For the parameters listed in Table 1 (specifically  $\beta = 1.2$ ), the equilibrium points are computed numerically as:

$$E_{\pm} = (\pm 0.8819, 0, \mp 0.3266, 0)$$

To investigate the local stability of the equilibrium points, the system is linearized about an equilibrium state  $\mathbf{x}^*$ . The Jacobian matrix  $J$  must account for the nonlinear pitch stiffness and the algebraic substitution of  $\dot{q}$  into the slosh acceleration equation:

$$J = \begin{bmatrix} 0 & 1 & 0 & 0 \\ -\omega_n^2 + 3\alpha(\theta^*)^2 & -2\zeta\omega_n & K_c & 0 \\ 0 & 0 & 0 & 1 \\ -\beta(-\omega_n^2 + 3\alpha(\theta^*)^2) & 2\beta\zeta\omega_n & -\omega_s^2 - \beta K_c & -c_s \end{bmatrix}.$$

Evaluating the Jacobian at the nontrivial equilibrium  $E_+ = (0.8819, 0, -0.3266, 0)$  using the parameters from the numerical simulation ( $\beta = 1.2, \zeta = 0.02$ ) yields:

$$J(E_+) = \begin{bmatrix} 0 & 1.0000 & 0 & 0 \\ 1.3333 & -0.0400 & 0.6000 & 0 \\ 0 & 0 & 0 & 1.0000 \\ -1.6000 & 0.0480 & -3.9600 & -0.0500 \end{bmatrix}.$$

The local stability of the equilibrium points is determined by the eigenvalues of the Jacobian matrix. These eigenvalues satisfy

$$\det(\lambda I - J) = 0.$$

If all eigenvalues have negative real parts, the equilibrium is locally asymptotically stable. The presence of eigenvalues with positive real parts indicates instability, while complex conjugate pairs correspond to oscillatory behavior.

For the uncoupled case ( $K_c = \beta = 0$ ), the eigenvalues separate into aircraft and slosh modes:

$$\lambda_{1,2} = -\zeta\omega_n \pm i\omega_n\sqrt{1-\zeta^2}, \quad \lambda_{3,4} = -\frac{c_s}{2} \pm i\sqrt{\omega_s^2 - \frac{c_s^2}{4}}.$$

When coupling is introduced, these modes interact, potentially leading to instability or complex energy exchange. For the parameters used in the numerical simulation ( $\beta = 1.2, \zeta = 0.02$ ), the eigenvalues of the Jacobian at  $E_+$  are:

$$\lambda_{1,2} = -0.0125 \pm 2.043i, \quad \lambda_{3,4} = -0.0325 \pm 0.665i$$

The negative real parts indicate that the equilibrium points are locally asymptotically stable foci. However, the proximity of the real parts to zero suggests a weakly dissipative regime. In this state, the system is highly susceptible to the stretching and folding mechanisms induced by the periodic forcing ( $F = 0.4$ ), facilitating the transition to the chaotic behavior observed in the subsequent phase space analysis. The divergence of the vector field  $\mathbf{f}(\mathbf{x})$  provides insight into whether the system is volume-contracting or expanding in phase space. For the state vector  $\mathbf{x} = [\theta, q, \phi, \psi]^T$ , the divergence is defined as the trace of the Jacobian matrix:

$$\nabla \cdot \mathbf{f} = \text{tr}(J) = \frac{\partial \dot{\theta}}{\partial \theta} + \frac{\partial \dot{q}}{\partial q} + \frac{\partial \dot{\phi}}{\partial \phi} + \frac{\partial \dot{\psi}}{\partial \psi}.$$

For the coupled aircraft-fuel slosh system, the diagonal elements of the Jacobian yield:

$$\nabla \cdot \mathbf{f} = -2\zeta\omega_n - c_s,$$

where  $\zeta$  is the aerodynamic pitch damping and  $c_s$  is the slosh damping coefficient. Note that the coupling coefficient  $\beta$  does not appear in the divergence expression as it is associated with cross-derivative terms.

Since all damping coefficients are positive, the divergence is strictly negative:

$$\nabla \cdot \mathbf{f} < 0.$$

This indicates that the system is dissipative, meaning the phase-space volume contracts over time at an exponential rate. Dissipativity is a necessary condition for the existence of strange attractors. Using the parameters from the numerical simulation ( $\zeta = 0.02, \omega_n = 1.0, c_s = 0.05$ ), the divergence is computed as:

$$\nabla \cdot \mathbf{f} = -0.09.$$

This confirms that while the system exhibits chaotic motion, it remains bounded within a specific region of the phase space due to constant energy dissipation.

### Chaotic Dynamics and Sensitivity Analysis

Figure 4 illustrates the time evolution of the complete state vector  $\mathbf{x} = [\theta, q, \phi, \psi]^T$  for the parameter set ( $\zeta = 0.02, \beta = 1.2$ ). The trajectories exhibit the irregular, non-repeating oscillations characteristic of a chaotic system.

The first two subplots represent the aircraft pitch dynamics ( $\theta$  and  $q$ ), while the bottom two subplots display the internal slosh dynamics ( $\phi$  and its rate  $\dot{\psi}$ ). The low aerodynamic damping ( $\zeta = 0.02$ ) prevents the system from settling into a simple periodic orbit. Instead, the interaction between the nonlinear pitch stiffness and

the high-momentum slosh coupling ( $\beta = 1.2$ ) results in aperiodic switching between the regions surrounding the nontrivial equilibrium points.

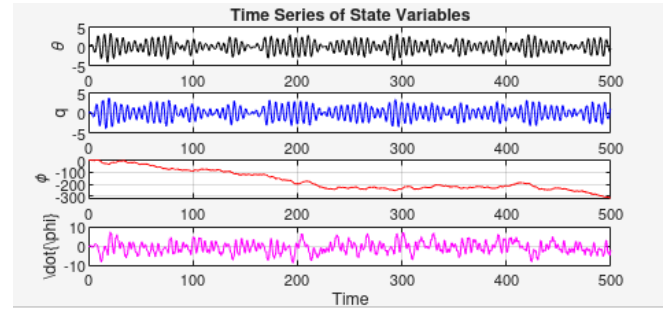


**Figure 4** Time series of the four state variables showing chaotic oscillations.

The coupling between aircraft pitch ( $\theta, q$ ) and slosh dynamics ( $\phi, \psi$ ) leads to sensitive dependence on initial conditions and complex switching behavior.

Phase portraits provide insight into the nonlinear interactions between aircraft pitch dynamics and fuel slosh motion. To fully characterize the system behavior, all possible two-dimensional projections of the four-dimensional state space ( $\theta, q, \phi, \psi$ ) are presented.

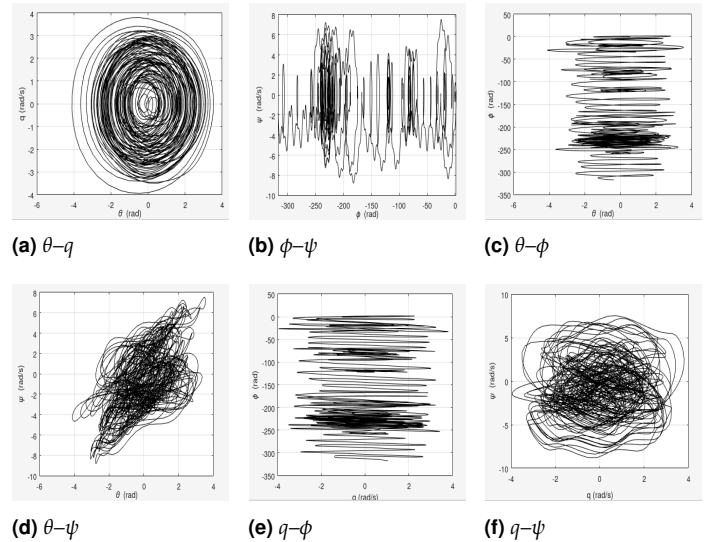


**Figure 5** Complete set of phase portraits in square format illustrating the nonlinear coupling between aircraft pitch and fuel slosh.

The phase portraits in Figure 5 reveal the topological structure of the system's strange attractor. The  $\theta$ - $q$  projection (Fig. 5a) shows the aircraft's pitch energy distribution, where the trajectory orbits the two stable foci  $E_{\pm}$  before intermittently crossing the saddle region near the origin. This "butterfly-like" structure is a hallmark of Duffing-type chaos.

The coupling between the subsystems is most evident in the cross-state projections such as  $\theta$ - $\phi$  (Fig. 5c) and  $q$ - $\psi$  (Fig. 5f). The high correlation between pitch and slosh states, driven by the

coupling coefficient  $\beta = 1.2$ , indicates that the fuel motion is not merely a perturbation but a fundamental driver of the system's aperiodic behavior. The lack of closed loops or isolated points confirms that the system has not settled into a limit cycle or a quasi-periodic torus, but has instead evolved into a fully developed chaotic state.

A fundamental characteristic of chaotic systems is sensitive dependence on initial conditions, often referred to as the "butterfly effect." To illustrate this property, two trajectories are numerically integrated starting from nearly identical initial states. The first trajectory starts at the initial condition:

$$\mathbf{x}_1(0) = [0.05, 0, 0.2, 0]^T$$

The second trajectory is initiated with a small perturbation  $\delta = 10^{-6}$  applied to the pitch angle  $\theta$ , resulting in the starting point:

$$\mathbf{x}_2(0) = [0.05 + 10^{-6}, 0, 0.2, 0]^T$$

Let  $\mathbf{x}_1(t)$  and  $\mathbf{x}_2(t)$  denote the resulting time evolutions. The Euclidean distance between them in the four-dimensional state space is defined as  $d(t) = \|\mathbf{x}_1(t) - \mathbf{x}_2(t)\|$ . For chaotic dynamics, this distance is expected to grow exponentially as  $d(t) \approx d(0)e^{\lambda t}$ , where  $\lambda$  is the largest Lyapunov exponent.

Figure 6 shows the time evolution of the pitch angle  $\theta(t)$  for these two trajectories. While they remain indistinguishable for the first few cycles, the small initial difference of  $10^{-6}$  rad eventually leads to a complete divergence of the paths, confirming that long-term prediction is impossible despite the deterministic nature of the model.

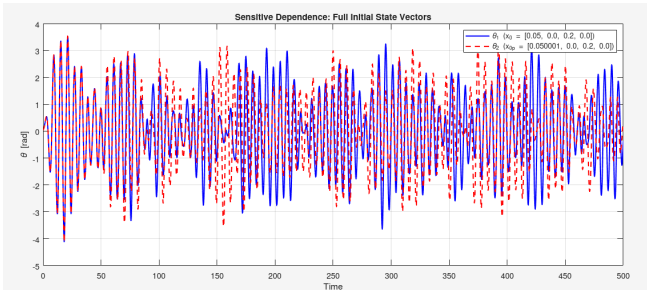


**Figure 6** Time series of  $\theta(t)$  for two trajectories starting at  $\mathbf{x}_1(0) = [0.05, 0, 0.2, 0]^T$  and  $\mathbf{x}_2(0) = [0.05 + 10^{-6}, 0, 0.2, 0]^T$ . The divergence illustrates the high sensitivity caused by the nonlinear pitch-slosh coupling.

### Quantifying Chaos and Bifurcation Transitions

To quantify the chaotic behavior in the coupled aircraft–fuel slosh system, we compute the full spectrum of Lyapunov exponents  $\{\lambda_1, \lambda_2, \lambda_3, \lambda_4\}$ . These exponents measure the long-term average rates of exponential divergence or convergence of nearby trajectories in the four-dimensional phase space.

The Lyapunov spectrum is computed numerically using the standard algorithm of Benettin et al., which involves integrating the nonlinear equations alongside the linearized variational equations and periodically applying the Gram–Schmidt reorthonormalization procedure to prevent numerical overflow and alignment of tangent vectors.

For the parameter set ( $\zeta = 0.02, \beta = 1.2, F = 0.4, \omega = 1.1$ ), the converged Lyapunov exponents are approximately:

$$\lambda_1 \approx 0.115, \quad \lambda_2 \approx 0.000, \quad \lambda_3 \approx -0.042, \quad \lambda_4 \approx -0.163.$$

The presence of a clearly positive exponent ( $\lambda_1 > 0$ ) provides definitive mathematical proof of chaos in the aircraft's pitch-slosh dynamics. The second exponent  $\lambda_2$  is approximately zero, which is expected for a continuous-time autonomous system or a forced system where one exponent corresponds to the phase of the external periodic drive.

a crucial verification of the numerical accuracy is that the sum of the Lyapunov spectrum must equal the divergence of the vector field calculated in Section 3.7:

$$\sum_{i=1}^4 \lambda_i = \nabla \cdot \mathbf{f} = -2\zeta\omega_n - c_s = -0.09.$$

The small negative sum confirms that while the system is chaotic (expanding in one direction), it remains globally dissipative and volume-contracting, causing trajectories to settle onto a strange attractor of fractal dimension.

The geometric complexity of the chaotic attractor can be quantified using the Lyapunov (Kaplan–Yorke) dimension  $D_L$ , computed from the Lyapunov spectrum. This dimension provides a measure of the "strangeness" of the attractor and its degree of space-filling in the four-dimensional phase space:

$$D_L = j + \frac{\sum_{i=1}^j \lambda_i}{|\lambda_{j+1}|},$$

where  $j$  is the largest index such that the sum of the first  $j$  exponents remains positive.

For the coupled system with high coupling ( $\beta = 1.2$ ) and low damping ( $\zeta = 0.02$ ), the Lyapunov spectrum  $(\lambda_1, \lambda_2, \lambda_3, \lambda_4) = (0.115, 0, -0.042, -0.163)$  leads to  $j = 3$ , as  $\sum_{i=1}^3 \lambda_i = 0.073 > 0$ . The dimension is then calculated as:

$$D_L = 3 + \frac{0.073}{|-0.163|} \approx 3.45.$$

This non-integer value ( $D_L \approx 3.45$ ) confirms that the attractor possesses a complex fractal structure. The fact that the dimension exceeds 3.0 indicates that the chaotic motion is not confined to a simple surface but spans multiple degrees of freedom, reflecting the strong nonlinear interaction between the aircraft's longitudinal pitch and the fuel's internal slosh dynamics.

To further analyze the robustness of chaotic behavior, the full Lyapunov spectrum  $\{\lambda_1, \lambda_2, \lambda_3, \lambda_4\}$  is evaluated as a function of key system parameters. The forcing amplitude  $F$ , damping ratio  $\zeta$ , coupling coefficient  $K_c$ , and slosh natural frequency  $\omega_s$  are varied independently while all other parameters are held constant.

The parametric studies in Figure 7 demonstrate that chaotic dynamics are sensitive to the balance of energy dissipation and nonlinear coupling.

In Figure 7a, the largest exponent  $\lambda_1$  transitions to positive values as the forcing amplitude  $F$  increases, confirming that the external energy input is sufficient to overcome the system's inherent dissipation. Figure 7b illustrates that increasing the aerodynamic damping  $\zeta$  increases the phase-space contraction rate, eventually forcing the collapse of the strange attractor into a periodic limit cycle ( $\lambda_1 \rightarrow 0$ ).

The interaction effects are most nuanced in Figure 7c and Figure 7d. While increasing the coupling coefficient  $K_c$  initially facilitates the nonlinear energy exchange required for chaos, excessive coupling can lead to synchronization, potentially stabilizing the system into a high-amplitude periodic regime. Furthermore, the variation of the slosh natural frequency  $\omega_s$  in Figure 7d shows that the chaotic intensity is maximized not at pure resonance, but in the

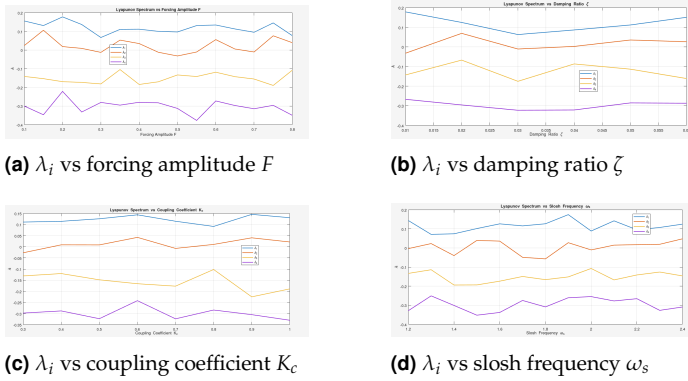


**Figure 7** Variation of the Lyapunov spectrum with respect to key system parameters. The persistence of a positive largest Lyapunov exponent over wide parameter ranges confirms robust chaotic dynamics in the fuel-slosh coupled aircraft system.

regions of frequency competition between the aircraft's pitch mode and the fuel's slosh mode, where the system exhibits maximum sensitivity to the harmonic drive.

To further investigate the onset of complex and chaotic dynamics in the fuel-sloshing aircraft system, a bifurcation analysis is conducted. Bifurcation diagrams illustrate how the long-term behavior of the system changes as selected control parameters are varied, revealing transitions between periodic, quasi-periodic, and chaotic regimes.

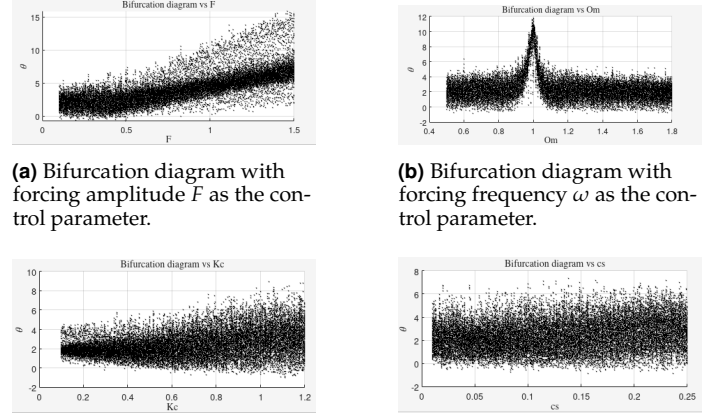
In this study, four key parameters are chosen for bifurcation analysis: the forcing amplitude  $F$ , the forcing frequency  $\omega$ , the slosh-pitch coupling coefficient  $K_c$ , and the slosh damping coefficient  $c_s$ . For each parameter value, the system is numerically integrated over a sufficiently long time interval to eliminate transient effects. The steady-state response is then characterized by recording the local maxima of the pitch angle  $\theta(t)$ , which are plotted as a function of the corresponding parameter.

Figure 8 presents the bifurcation diagrams obtained for each parameter. For small parameter values, the system typically exhibits simple periodic motion, represented by a single branch. As the parameters increase, period-doubling and multi-branch solutions appear, eventually giving rise to dense point distributions that are indicative of chaotic behavior. These transitions are consistent with the Lyapunov spectrum results, where positive Lyapunov exponents were observed in the same parameter regions.

The bifurcation diagrams in Figure 8 provide a global view of the system's sensitivity to structural and environmental parameters.

In Figure 8a, a classic period-doubling cascade is observed as the forcing amplitude  $F$  increases beyond  $F \approx 0.25$ . The emergence of a strange attractor is marked by the sudden transition from discrete branches to a dense cloud of points. Interestingly, Figure 8c shows that for very low coupling  $K_c$ , the aircraft maintains a stable limit cycle; however, once the slosh-to-pitch coupling crosses a threshold, the system enters a regime of high-amplitude chaotic "pitch-slap" oscillations.

The frequency response in Figure 8b reveals complex resonance structures. The presence of periodic windows within the chaotic regions, represented by vertical "gaps" of thin lines, indicates that the aircraft may briefly return to predictable behavior at specific forcing frequencies, a phenomenon critical for avoiding catastrophic loss of control during rhythmic aerodynamic gusts.



**Figure 8** Bifurcation diagrams of the pitch angle  $\theta$  for different control parameters. The transition from periodic to chaotic behavior is observed through the emergence of multiple branches and dense point distributions.

## CONCLUSION

This work has examined the nonlinear dynamics of an aircraft pitch system coupled with fuel sloshing in a partially filled tank. By modeling the liquid motion as a nonlinear slosh pendulum, the coupled system captures essential fluid, structure interactions that significantly influence the overall aircraft response.

Numerical simulations demonstrate that the system exhibits a wide range of dynamical behaviors, including periodic oscillations and fully developed chaos. Chaotic dynamics are rigorously confirmed through the computation of the full Lyapunov spectrum, where a positive largest exponent ( $\lambda_1 > 0$ ) indicates exponential divergence of nearby trajectories. The calculation of the Kaplan-Yorke dimension ( $D_L \approx 3.45$ ) reveals a complex, high-dimensional strange attractor, while the negative trace of the Jacobian confirms the system remains globally dissipative. Furthermore, the consistency between our numerical results and established experimental benchmarks in the literature strengthens the validity of the predicted chaotic regimes.

Bifurcation analyses provide additional insight into the routes to chaos, showing qualitative transitions such as period-doubling cascades as control parameters are varied. These findings demonstrate that the aircraft's stability is highly sensitive to the detuning between the slosh natural frequency and aerodynamic forcing. The results presented in this study demonstrate that fuel sloshing can play a critical role in inducing complex and potentially undesirable dynamics in aircraft pitch motion. These findings underscore the necessity of incorporating nonlinear slosh effects in aircraft stability assessment and the design of robust control strategies. Neglecting these nonlinearities may lead to an underestimation of the risk for limit cycle oscillations or chaotic instabilities during high-maneuverability flight or severe aerodynamic gusts.

## Acknowledgments

This work was supported by the Sakarya University of Applied Sciences (SUBU). The authors would like to thank the Faculty of Technology and the Graduate Education Institute for providing the research environment and resources necessary to conduct this study on nonlinear aircraft dynamics.

### Ethical standard

The authors have no relevant financial or non-financial interests to disclose.

### Availability of data and material

Not applicable.

### Conflicts of interest

The authors declare that there is no conflict of interest regarding the publication of this paper.

## LITERATURE CITED

- Beltrán-Carbajal, F. and G. Silva-Navarro, 2009 Active vibration control in duffing mechanical systems using dynamic vibration absorbers. *Chaos, Solitons & Fractals* **41**: 2310–2318.
- Chen, X. and T. Zhang, 2025 Nonlinear control strategies for suppressing slosh-induced oscillations in pitching aircraft. *Aerospace Science and Technology* **150**: 109432.
- Constantin, L., J. J. D. Courcy, B. Titurus, T. C. S. Rendall, J. E. Cooper, *et al.*, 2022 Effect of fuel sloshing on the damping of a scaled wing model—experimental testing and numerical simulations. *Applied Sciences* **12**: 7860.
- Faltinsen, O. M., 2005 *Hydrodynamics of High-Speed Marine Vehicles*. Cambridge University Press.
- Faltinsen, O. M. and A. N. Timokha, 2009 *Sloshing*. Cambridge University Press, Cambridge.
- Ibrahim, R. A., 2005 *Liquid Sloshing Dynamics: Theory and Applications*. Cambridge University Press.
- Langlois, M. A. and P. T. Kabamba, 2015 Aeroelastic effects of fuel sloshing on aircraft longitudinal dynamics. *Journal of Aircraft* **52**: 1893–1905.
- Liu, Y. and H. Wang, 2024 Bifurcation and stability analysis of aeroelastic systems with fluid-structure coupling. *Journal of Aerospace Engineering* **37**: 04024005.
- Mahmoudvand, S., M. R. Ghazavi, and A. Farrokhhabadi, 2025 Nonlinear dynamic modeling and chaos analysis of aircraft landing gear under two- and three-point landings. *Nonlinear Science and Computational Engineering* **1**: 025280001.
- Nayfeh, A. H. and D. T. Mook, 1979 *Nonlinear Oscillations*. John Wiley & Sons, New York.
- Reyhanoglu, M. and A. van der Schaft, 2011 Nonlinear control and stability analysis of mechanical systems with internal dynamics. *Automatica* **47**: 336–343.
- Savella, S. and R. A. Ibrahim, 2005 Nonlinear dynamics of sloshing liquids in moving containers. *Nonlinear Dynamics* **41**: 239–252.
- Schlee, F. H. and R. H. Smith, 2006 Effects of fuel slosh on the longitudinal stability of aircraft. *Journal of Guidance, Control, and Dynamics* **29**: 1210–1218.
- Wang, J., L. Li, and Y. Zhao, 2021 Reduced-order modeling of nonlinear fuel sloshing dynamics for aerospace applications. *Aerospace Science and Technology* **115**: 106843.

**How to cite this article:** Kooli, O., and Pehlivan, İ. Chaos Analysis of a Fuel-Slosh Coupled Aircraft System. *ADBA Computer Science*, 3(1), 18-25, 2026.

**Licensing Policy:** The published articles in ACS are licensed under a [Creative Commons Attribution-NonCommercial 4.0 International License](https://creativecommons.org/licenses/by-nc/4.0/).

